JOURNAL OF VIROLOGY, Oct. 2007, p. 11363–11371 Vol. 81, No. 20
0022-538X/07/$08.00+0 doi:10.1128/JVI.01281-07

Pseudorabies Virus Us9 Directs Axonal Sorting of Viral Capsids▽†

M. G. Lyman,[1] B. Feierbach,[1,2] D. Curanovic,[1] M. Bisher,[1] and L. W. Enquist[1]*

Department of Molecular Biology, Princeton University, Princeton, New Jersey 08544,[1] and Lewis-Sigler Institute for Integrative Genomics, Princeton, New Jersey 08544[2]

Received 12 June 2007/Accepted 31 July 2007

Pseudorabies virus (PRV) mutants lacking the Us9 gene cannot spread from presynaptic to postsynaptic neurons in the rat visual system, although retrograde spread remains unaffected. We sought to recapitulate these findings in vitro using the isolator chamber system developed in our lab for analysis of the transneuronal spread of infection. The wild-type PRV Becker strain spreads efficiently to postsynaptic neurons in vitro, whereas the Us9-null strain does not. As determined by indirect immunofluorescence, the axons of Us9-null infected neurons do not contain the glycoproteins gB and gE, suggesting that their axonal sorting is dependent on Us9. Importantly, we failed to detect viral capsids in the axons of Us9-null infected neurons. We confirmed this observation by using three different techniques: by direct fluorescence of green fluorescent protein-tagged capsids; by transmission electron microscopy; and by live-cell imaging in cultured, sympathetic neurons. This finding has broad impact on two competing models for how virus particles are trafficked inside axons during anterograde transport and redefines a role for Us9 in viral sorting and transport.

Pseudorabies virus (PRV) is a neurotropic alphaherpesvirus closely related to the human pathogens herpes simplex virus (HSV) and varicella-zoster virus (23). These viruses are parasites of the mammalian nervous system and initially invade sensory and autonomic neurons that innervate the primary site of infection—normally an epithelial cell layer. The transport of virus particles to and from the cell body is dependent on microtubule-based motors, including the dynein motor complex for minus-end directed movement (retrograde) and a kinesin family motor for plus-end directed movement (anterograde) (24).

PRV infects and spreads within the peripheral and central nervous systems in a wide range of mammals and is commonly used to map neuronal circuitry in the brain (12). Previous work in our lab has identified three PRV gene products—gE, gI, and Us9—that are critical for anterograde spread of infection in synaptically connected neurons (13); deletion of any one of these three genes reduces viral spread from presynaptic to postsynaptic neurons, but not vice versa (3, 9). The PRV Us9 gene product is a phosphorylated, type II membrane protein that is "tail anchored," meaning that it has no identifiable signal sequence and has an amino terminus that resides in the cytosol and a carboxy-terminal anchor that spans the lipid bilayer (2). Its steady-state concentration is highest in or near the *trans*-Golgi network (2). The Us9 protein also contains an acidic cluster motif responsible for its endocytosis from the plasma membrane (4). The absence of Us9 does not affect cell-to-cell spread in Madin-Darby bovine kidney cells but has a dramatic effect on the anterograde spread of infection in the visual circuitry of the rat brain and neuron-to-cell spread in vitro, suggesting that Us9 performs a neuron-specific function during replication (3, 10). Tomishima and Enquist reported that PRV Us9 was essential for the axonal sorting of viral glycoproteins but not capsid or tegument proteins (28). This finding strongly supported the notion that viral capsids and membranes trafficked separately in the axon during anterograde transport.

In the present study we report that Us9 is, in fact, necessary for the anterograde transport of viral capsids as well as viral glycoproteins. Our data support recent studies indicating that viral capsids and glycoproteins traffic together during anterograde transport in axons, likely as an enveloped or partially enveloped virus particle inside a secretory vesicle.

MATERIALS AND METHODS

Cells and virus. Porcine kidney cells (PK15) were maintained at 37°C in Dulbecco modified Eagle medium supplemented with 10% fetal bovine serum and Pen/Strep (HyClone) in a 5% CO_2 environment. All PRV strains were propagated on PK15 cells at a low multiplicity of infection for 48 h and then collected by scraping cells into the conditioned medium. To normalize the pH of the virus sample, sterifiltered 1 M HEPES buffer was added to a final concentration of 10 mM before freezing aliquots at −80°C. The wild-type PRV strain Becker and its derivatives PRV 160, PRV GS443, PRV 368, and PRV 180 were described previously (3, 6, 11, 25, 28). PRV 160 (Us9-null) contains a nonsense stop mutation at position 4 in the Us9 open reading frame. GS443 expresses green fluorescent protein (GFP) fused to the capsid protein VP26. PRV 368 was constructed by recombination between PRV 160 and GS443, yielding a Us9-null virus expressing GFP-VP26. PRV 180 expresses red fluorescent protein (RFP) fused to the capsid protein VP26.

Antibodies. The antibodies used here include polyclonal rabbit antiserum recognizing the gE cytoplasmic domain (27) (used at 1:400 by immunofluorescence [IF]), polyclonal goat antiserum recognizing gB (31) (used at 1:200 by IF), mouse monoclonal antibody to PRV major capsid protein (made by Alex Flood at the Princeton Monoclonal Antibody Facility; used at 1:100 for IF). All secondary Alexa fluorophores (used at 1:500) were purchased from Molecular Probes.

Neuronal cultures. Detailed protocols for dissecting and culturing neurons are found in Ch'ng et al. (8). Briefly, sympathetic neurons from the superior cervical ganglia were dissected from embryonic day 15.5 (E15.5) to E16.5 pregnant Sprague-Dawley rats (Hill-Top Labs, Inc., Pennsylvania) cut in half with dissection knives and plated within a 35-mm plastic tissue culture dish on top of a square of Aclar (Electron Microscopy Sciences, Pennsylvania) coated with 500

* Corresponding author. Mailing address: 314 Schultz Laboratory, Department of Molecular Biology, Princeton University, Princeton, NJ 08544. Phone: (609) 258-2415. Fax: (609) 258-1035. E-mail: lenquist@princeton.edu.

† Supplemental material for this article may be found at http://jb.asm.org/.

▽ Published ahead of print on 8 August 2007.

μg of poly-DL-ornithine (Sigma Aldrich)/ml diluted in borate buffer and 10 μg of natural mouse laminin (Invitrogen)/ml. The neuron culture medium consists of Dulbecco's modified Eagle medium (Invitrogen) and Ham F-12 (Invitrogen) in a 1:1 ratio. The serum-free medium was supplemented with 10 mg of bovine serum albumin (BSA; Sigma Aldrich)/ml, 4.6 mg of glucose (J. T. Baker)/ml, 100 μg of holotransferrin (Sigma Aldrich)/ml, 16 μg of putrescine (Sigma Aldrich)/ml, 10 μg of insulin (Sigma Aldrich)/ml, 2 mM L-glutamine (Invitrogen), 50 μg/ml or units of penicillin and streptomycin (Invitrogen), 30 nM selenium (Sigma Aldrich), 20 nM progesterone (Sigma Aldrich), and 100 ng of nerve growth factor 2.5S (Invitrogen)/ml. At 2 days postplating, the neuronal cultures are treated with a 1 M concentration of an antimitotic drug called cytosine-D-arabinofuranoside (Sigma-Aldrich) to eliminate any non-neuronal cells. The neuron culture medium was replaced every 3 days, and cultures were kept in a humidified, CO_2-regulated 37°C incubator. At 6 days postplating SCG explants, a Teflon chamber (see below for details) was placed adjacent to the explant, so as to capture axons and their growth cones. All experimental protocols related to animal use have been approved by the Institutional Animal Care and Use Committee of the Princeton University Research Board under protocol number 1453-AR2 in accordance with the regulations of the American Association for Accreditation of Laboratory Animal Care and those in the Animal Welfare Act (Public Law 99-198).

Chamber culture system. This system was described previously by Feierbach et al. (15). Briefly, Teflon rings were purchased from Tyler Research (Alberta, Canada), and protocols were modified from previously published reports for Campenot chambers. All tools and reagents including the Teflon rings and silicone grease-loaded syringe (Dow Corning) were sterilized via autoclaving prior to assembly. A 10-ml disposable syringe attached to a truncated P200 pipette tip was filled with silicone grease. Using the silicone grease-loaded syringe, a thin, continuous strip of silicone grease was applied over the entire bottom surface of a Teflon ring. The silicone grease-coated ring was placed into the media and gently dropped over the 1-week-old explant axons, adjacent to the explant cell bodies. The ring was allowed to settle by gravity over the axons and make contact with the surface of the Aclar. When we tested transneuronal spread, we placed dissociated superior cervical ganglia neurons (approximately one-fourth of a single ganglion, which results in approximately 5,000 cell bodies) inside the ring the following day. Neuron cultures were maintained according to established protocols stated in the previous section.

Indirect IF. Explants and dissociated neurons were grown on the surface of a flexible thermoplastic fluoropolymer film known as Aclar (EM Sciences). Aclar is biochemically inert and exhibits no detectable autofluorescence. The Aclar was cut into squares that fit inside a 35-mm plastic tissue culture dish and were UV sterilized for 20 min. After sterilization, the Aclar squares were coated with poly-DL-ornithine and laminin, and SCG explants were plated directly upon the Aclar surface. All subsequent neuron culture and viral infection protocols are similar to those described in previous sections. Chambers were infected in duplicate for each virus strain tested. To fix the neurons both inside and outside the chamber, the medium was carefully removed, washed with phosphate-buffered saline (PBS), and replaced with 4% paraformaldehyde in PBS. Neurons were fixed for 10 min in the dark. After fixation, the chamber was carefully lifted from the Aclar, and the remaining silicone grease was gently cleared without disrupting the fixed cells. The Aclar surface was then washed with PBS, followed by a wash with PBS containing 3% BSA, and permeabilized by PBS with BSA and 0.5% Triton X-100 for 3 to 5 min. After permeabilization, primary antibodies were added for 1 h. After the primary antibodies were removed, the sample was washed three times with PBS with BSA and 0.5% saponin. Next, secondary antibodies were added to the sample and incubated for 1 h. Secondary antibodies were then removed, and the sample was washed three times with PBS with BSA and 0.5% saponin. Samples were mounted on a glass slide by using Aqua Poly/Mount (Polysciences) and a coverslip was placed on top of the sample. The slide was air dried for 24 h prior to imaging.

Confocal microscopy and live imaging. Fixed samples were imaged with a Perkin-Elmer RS3 spinning disk confocal microscope side-mounted on a TE200-S Nikon Eclipse microscope with an argon-krypton laser producing excitation lines of 488, 568, and 647 nm. Optical sections were acquired in 0.5-μm steps. Two-dimensional projections of confocal stacks and channel merges were created by ImageJ 1.32j software (National Institutes of Health). Live imaging of viral capsids was performed on the Leica SP5 with a 40X 1.3 NA oil objective. Prior to imaging, 1 M HEPES was added to the medium to a final concentration of 25 mM. Neurons were cultured on MatTek Corp. glass-bottom dishes. The dish was warmed to 37°C by using a DH40i Micro-Incubation System (Warner Instrument Corp.) run at constant voltage (~5.5 V). Laser lines at 488 and 561 nm were used for individual and simultaneous GFP/RFP excitation, with emissions from 495 to 553 nm and from 587 to 702 nm collected for GFP and RFP, respectively. Images were acquired by using a 2.0 airy unit detector pinhole and scanning at 700 Hz. A minimum of 30 infected neurons (per virus) were examined for the presence of capsid puncta moving in the anterograde direction, including neurons coinfected with PRV 180 and PRV 368. In order to quantify the number of puncta undergoing axonal transport in neurons infected with PRV GS443, eight different axon shafts were imaged where capsids could be visualized moving >50 μm without dropping in and out of the plane of focus. An equal number of axons were examined for PRV 368 for the same time period. All figures were assembled in Adobe Photoshop 7.0.1.

Electron microscopy. The chamber was assembled on Aclar (EM Sciences) as described above, and SCG explants (outside of the chamber) were infected at a high multiplicity of infection. At 24 h postinfection, chambers were washed twice with PBS, fixed with 2% glutaraldehyde in 0.2 M sodium cacodylate buffer (pH 7.2) for 4 h, and postfixed with 1% osmium tetroxide in sodium Veronal buffer for 1 h on ice. Samples were then rinsed with sodium Veronal buffer four times and incubated with 0.25% toluidine blue in 0.2 M cacodylate buffer (pH 7.2) for 1 h; the staining solution was then removed with four rinses of sodium Veronal buffer (pH 7.2), followed by four rinses with 0.05 M sodium maleate buffer (pH 5.1). Overnight incubation with 2% uranyl acetate in 0.05 M sodium maleate buffer was done in the dark, followed by four rinses with 0.05 M sodium maleate buffer (pH 5.1). The fixed samples (done in duplicate) were then dehydrated with ethyl alcohol and embedded in Epon resin (EM Sciences). A 1-mm square inside the chamber (with high axonal density) was selected for serial sectioning. The selected area was cut into six 70-nm sections using a Leica UC-6 ultramicrotome and examined by using a Leo 912AB transmission electron microscope operated at 80 kV. Removal of the chamber from the Aclar leaves behind a visible layer of grease that serves as a chamber "footprint." This mark aids in determining areas inside and outside the chamber wall.

RESULTS

We have studied extensively the directional, transneuronal spread of PRV in the rat visual system (6, 7). In these studies, virus is injected into the vitreous humor of the rat eye where it infects retinal ganglion cells. Infection then spreads in an anterograde fashion (presynaptic to postsynaptic neurons) to all regions of the brain that receive retinal input. Immunohistochemical staining of viral antigens is then performed on sliced, fixed tissue from infected animals, typically a tedious process. Feierbach et al. recently reported the use of a facile in vitro chamber system that recapitulates the transneuronal spread phenotypes of several PRV mutants (15). Ganglion explants are plated and allowed to extend axons for 1 week. A nonseptated, Teflon chamber disk is placed on top of the axons thereby capturing a subpopulation of axon ends. Dissociated neurons are then plated inside the chamber ring and allowed to form connections with the explant axon termini. Thus, an isolated population of both presynaptic and postsynaptic neurons can be established.

We have reported that deleting Us9 precludes anterograde, transneuronal spread through anterograde circuits in vivo, while trafficking through retrograde circuits is unaffected (3). To test whether a Us9-null mutant was unable to spread from primary to second-order neurons using the in vitro chamber system, we infected the SCG explant on the outside of the chamber either with wild-type PRV Becker or with Us9-null mutants. After 24 h, the dissociated SCG neurons inside the chambers were examined by indirect IF (illustrated in Fig. 1A). After infection with PRV Becker, >70% of second-order neurons inside the chamber reacted readily with antiserum specific for viral glycoproteins gE and gB, as well as the major capsid protein VP5 (Fig. 1B, top row). This was determined by calculating the number of immunopositive cell bodies as a ratio to the total number of cell bodies in a field of view ($n = 20$). In contrast, when explants were infected with the Us9-null virus,

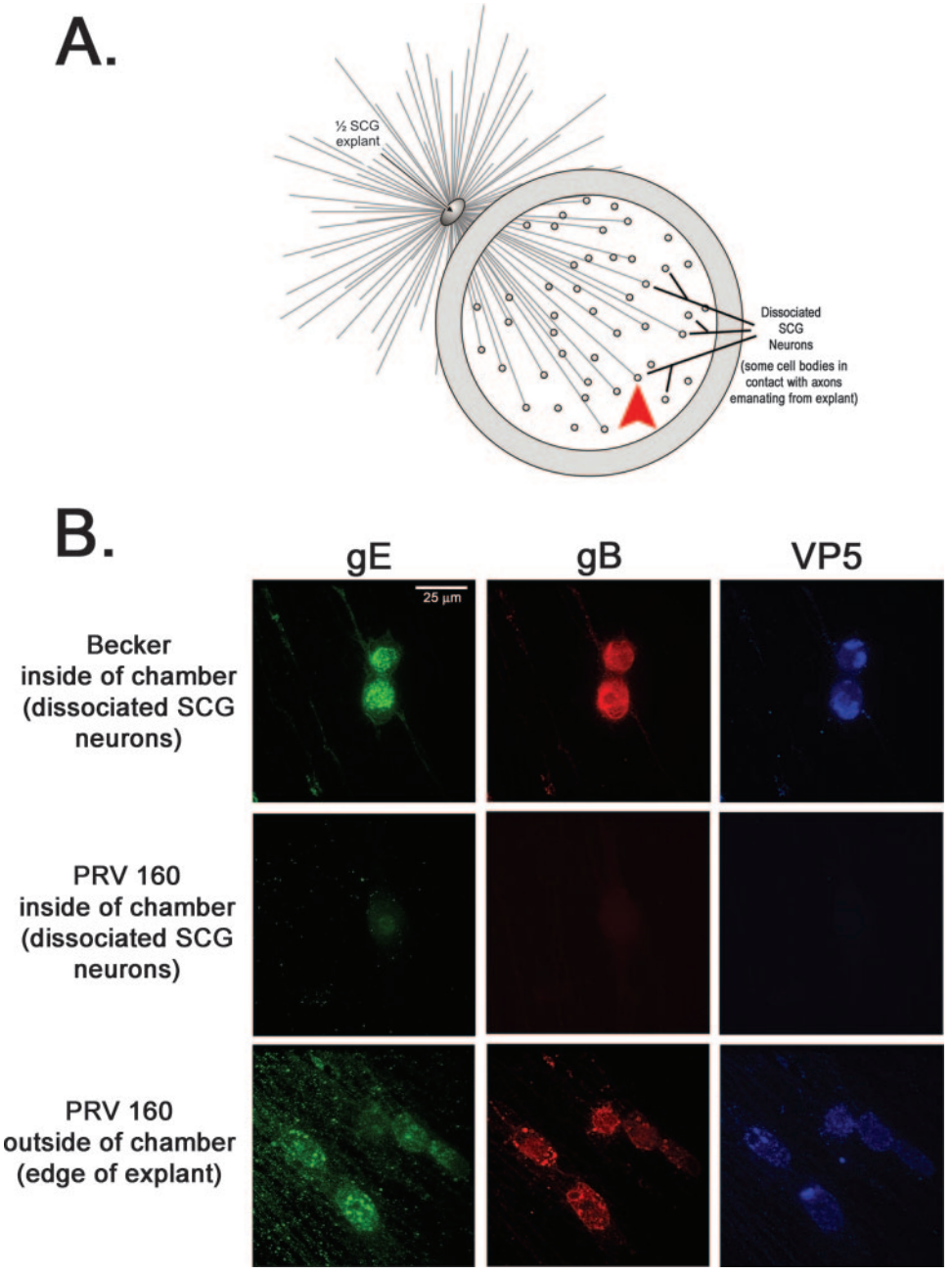

FIG. 1. Us9 is essential for transneuronal spread in vitro. (A) Diagram illustrating the isolator chamber system in which one-half of an SCG explant is plated on Aclar and allowed to extend neurites. A Teflon chamber ring is then placed on top of preformed axons, capturing a subpopulation of axon ends. Dissociated SCG neurons are then plated inside the chamber, where they mature and form synaptic connections with axons emanating from the explant. Dissociated SCG neurons inside the chamber are equivalent to one-fourth of an SCG ganglia, which is approximately 5,000 neurons. All chambers were prepared in duplicate. The red arrowhead denotes where the images in panel B were taken in reference to the SCG explant. (B) Explants were infected on the outside of the chamber with wild-type PRV Becker or PRV 160 (Us9-null). At 24 h postinfection, both the explant and the dissociated neurons inside the chamber were fixed and labeled with antibodies that recognize the viral glycoproteins gE and gB, as well as the major capsid protein VP5. Postsynaptic neurons in contact with the Becker-infected SCG explant stained for viral glycoprotein and capsid proteins (top row). No labeling of viral antigen was detected in postsynaptic neurons in contact with the explant infected with PRV 160 (middle row), although the explant itself showed extensive infection (bottom row).

dissociated neurons inside the chamber ring showed no reactivity with gE, gB, or VP5 (Fig. 1B, middle row). However, Us9-null mutants were capable of efficient infection of explant neurons as determined by strong reactivity with antiserum against gE, gB, and VP5 (Fig. 1B, bottom row). We did note a uniform, nonspecific "speckle" pattern in some samples labeled with the anti-gE antibody. This pattern was present in mock-infected cells and corresponded to areas of high cell density (e.g., near the SCG explant). However, it was not a confounding factor in the interpretation of our results. Overall,

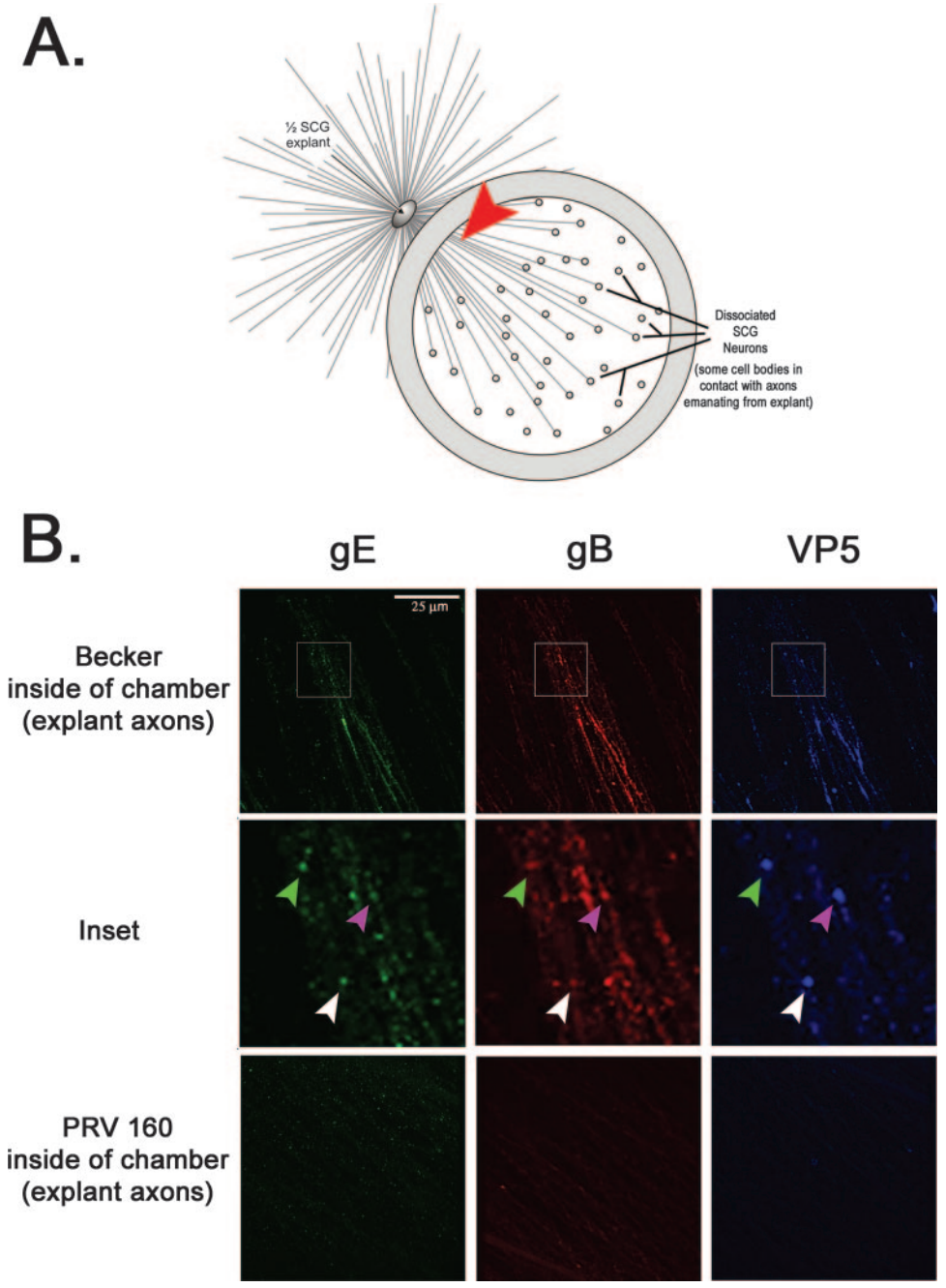

FIG. 2. Axonal sorting of viral capsid and membrane proteins is dependent on Us9. All samples were prepared and imaged in duplicate. (A) Presynaptic axon shafts were imaged directly inside the chamber ring (denoted by the red arrowhead). (B) Explants were infected with PRV Becker and PRV 160 for 24 h and then fixed and labeled with antibodies that recognize gE, gB, and VP5. A minimum of 20 fields were analyzed at a high magnification (×60). Axons emanating from Becker-infected explants showed strong labeling for both viral capsid and glycoproteins (top row, inset). Explants infected with PRV 160 did not have any labeling above background fluorescence (bottom row). It is noteworthy that there were no observable gradations in staining with the Us9-null mutant; viral proteins were not detected inside the chamber.

these findings are consistent with the inability of Us9-null infections to spread through anterograde circuitry of the rat visual system (3).

Tomishima and Enquist speculated that the Us9 transneuronal spread phenotype reflected the lack of sorting of viral glycoproteins into the axon of infected neurons. However, they reported that in Us9-null infections, capsids, and tegument proteins entered the axon unimpeded (28). To confirm the finding in our in vitro chamber system, we imaged the axon shafts emanating from the SCG explant physically isolated inside the chamber ring (Fig. 2A, arrowhead). Axons originating from Becker-infected explants showed strong reaction with antisera specific for gE, gB, and VP5 (Fig. 2B, top row). Some puncta labeled with VP5 antibody also costained with gE and

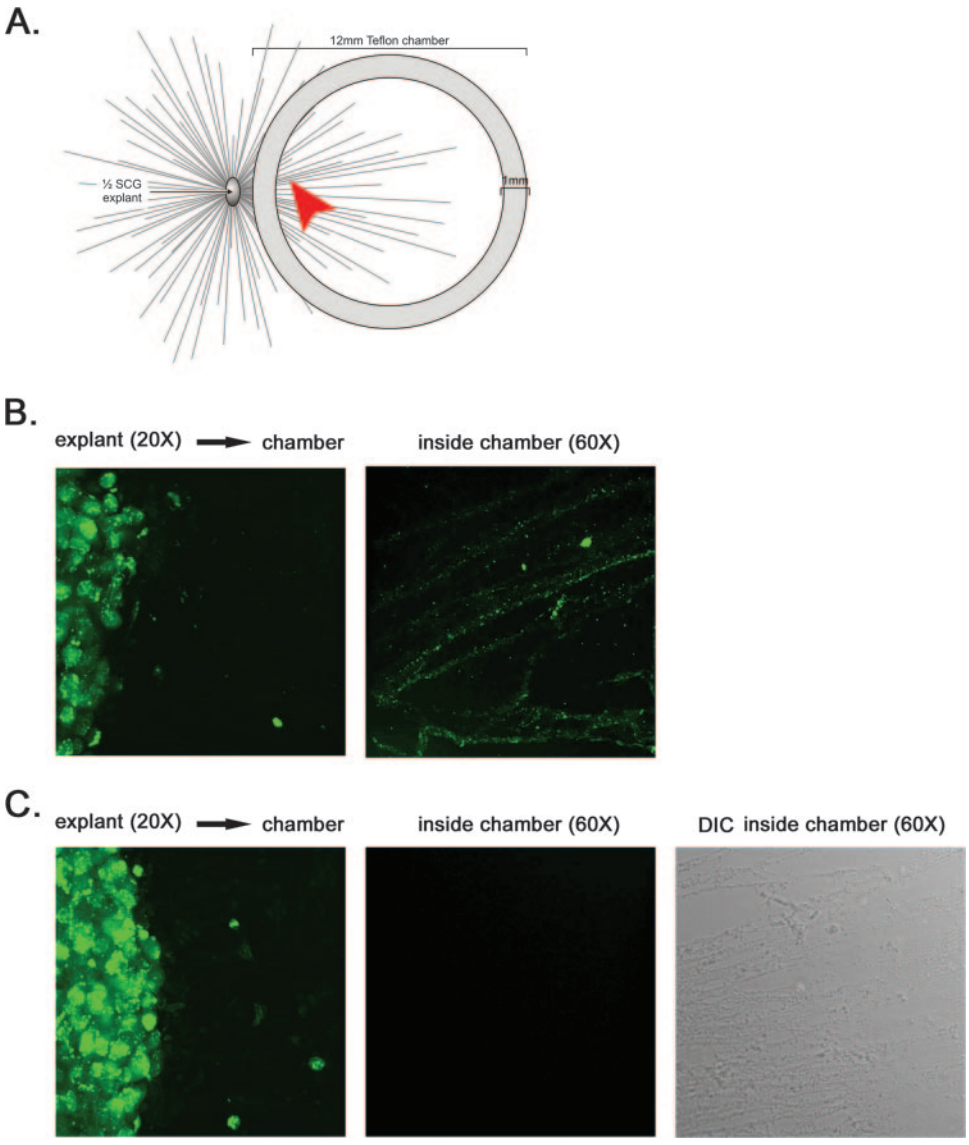

FIG. 3. GFP-tagged capsids do not enter the axon in the absence of Us9. (A) A chamber ring was placed on top of preformed axons emanating from the SCG explant to physically separate the site of infection from the site of imaging. No dissociated SCG neurons were plated inside the chamber. The arrowhead highlights the region where images were taken at high magnification within the chamber. (B and C) Explants were infected for 24 h with PRV GS443 (GFP-VP26) (B) or PRV 368 (GFP-VP26, Us9 null) (C) and fixed with 4% paraformaldehyde. Direct fluorescence of explants outside the chamber (×20 magnification) and capsids inside the chamber (×60 magnification) was visualized by using spinning-disk confocal microscopy.

gB antisera, suggesting that capsids were transported together with viral glycoproteins (Fig. 2B, inset). In contrast, axons originating from explants infected with the Us9-null mutant did not react with antisera against gE or gB, which is consistent with previous observations (28). Surprisingly, we did not detect any reaction with VP5 antibodies, suggesting that sorting of viral capsids into axons is, in fact, dependent on Us9 (Fig. 2B, bottom row).

To confirm and extend these unexpected findings, we first infected SCG explants on the outside of the chamber with PRV GS443, a recombinant PRV strain that expresses GFP fused to VP26, a capsid protein (25). This fusion protein efficiently assembles into capsids that can be visualized as uniform green puncta in live imaging and fixed preparation studies. We and others have used PRV GS443 for assessing capsid trafficking kinetics in axons (25), virus particle composition during anterograde and retrograde transport (1), and actin/assembly body formation in the nucleus of infected neurons (16). After 24 h, capsid puncta had traveled from the explant and were readily detected in axons inside the chamber (Fig. 3B). Importantly, when explants were infected with PRV 368, a GFP-VP26-expressing mutant with Us9 deleted, no green puncta were detected inside the chamber, although an extensive network of axons was visible (Fig. 3C). This was determined by analyzing multiple fields of view ($n = 20$) of duplicate samples at high magnification.

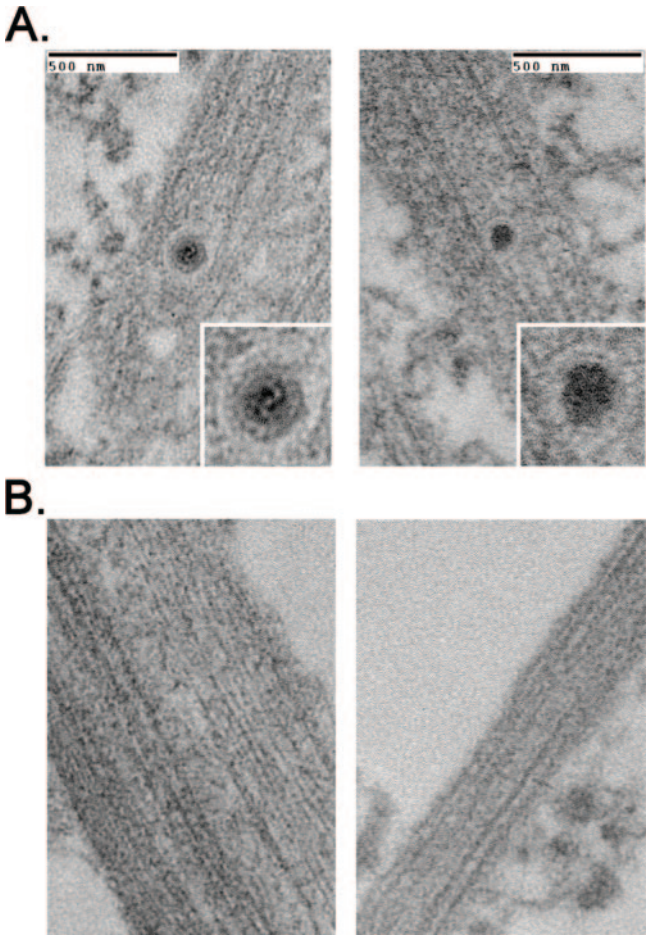

FIG. 4. Axons are devoid of enveloped virus particles during a Us9-null infection. Explants on the outside of the chamber were infected for 24 h with PRV Becker or PRV 160 (Us9-null), and axons inside the chamber were visualized by transmission electron microscopy. Samples were examined in duplicate. A 1-mm square with high axonal density inside the chamber was selected for sectioning by the ultramicrotome. Six serial sections (70 nm apart) were scrutinized for the presence of virus particles. (A) Enveloped virus particles were detected in the distal-axon of Becker-infected explants but were not present in explants infected with PRV 160 (B).

We next used transmission electron microscopy to determine whether capsids were present in the distal axons of infected explants. Explants on the outside of the chamber were infected with PRV Becker or a Us9-null mutant and then imaged directly inside the chamber ring 24 h postinfection. Capsids were detected readily in the distal axons of explants infected with PRV Becker. All were found within a membranous vesicle and contained a proteinaceous tegument layer juxtaposed to the capsid (Fig. 4A). This morphology is consistent with other ultrastructural studies examining PRV infection of primary neurons and tissue culture cells (15, 17, 30). Importantly, when explants were infected with the Us9-null mutant, no capsid structures could be detected inside the chamber ring despite an extensive search (Fig. 4B).

We next used a live-cell imaging approach in order to quantify the number of capsids moving in the axons of dissociated SCG neurons (as deduced by GFP-VP26 puncta visible in the confocal microscope). This technique enabled us to distinguish GFP-VP26 puncta moving by fast-axonal transport in the anterograde or retrograde direction from those that were not moving or from background fluorescence. Dissociated neurons were infected with PRV GS443 or PRV 368 and imaged between 13 and 14 h postinfection. A total of 128 GFP-VP26 puncta were observed moving in the anterograde direction in PRV GS443-infected neurons, entering the field of view by, on average, 4.6 $\pm$ 1.6 capsids/min (Fig. 5A; see also Movie S1 in the supplemental material). Despite extensive analyses, no capsid puncta were observed in the axon of neurons infected with PRV 368, although GFP-VP26 signal was clearly visible in the soma (Fig. 5B; see also Movie S2 in the supplemental material). To test whether the axonal sorting defect in PRV 368 was due to the lack of Us9 protein, we coinfected neurons with PRV 368 and PRV 180 (a Becker recombinant expressing mRFP-VP26) (11). We could easily detect green, red, and yellow puncta moving in the anterograde direction in coinfected neurons (Fig. 6 and see also Movie S3 in the supplemental material). We conclude that PRV 368-infected neurons can sort and move GFP-VP26 capsid puncta in their axons when complemented in *trans* by a Us9-expressing virus recombinant.

DISCUSSION

We report here that the axonal targeting of PRV capsids is dependent on the viral membrane protein Us9. We confirmed this observation by indirect IF (Fig. 2), direct fluorescence of GFP-tagged capsids (Fig. 3), transmission electron microscopy (Fig. 4), and live-cell imaging in cultured, sympathetic neurons (Fig. 5 and 6). Our findings raise a key question: why did we obtain such disparate results using essentially the same reagents as Tomishima and Enquist (14, 28)? In short, the answer is that imaging the proximal axon of infected neurons, as was done in the previous studies, can be misinterpreted, particularly when indirect IF is used at late times after infection. For example, Tomishima and Enquist fixed neurons infected with PRV GS443 and PRV 368 at 17 hpi and used anti-EGFP antibodies to enhance GFP signal in axons (28). We believe that the signal observed by Tomishima and Enquist was unassembled GFP-VP26 protein and not assembled capsids. This free GFP-VP26 in the proximal axon confounded interpretation of "capsid" localization in axons infected with a Us9-null virus, especially when images were obtained at low magnification (14, 28). We first came to this idea from live neuron imaging studies with PRV GS443 and PRV 368. We consistently observed a diffuse green fluorescent signal building in the proximal axon late in infection (>12 h postinfection). Indeed, by 16 h postinfection, this diffuse signal was strong enough in the proximal segment that we could visualize the connection of cell bodies to cognate axons. The general phenomenon of entry of unassembled structural proteins into the proximal segment of axons during infection also may explain the bright, but noticeably diffuse signal of the major capsid protein VP5 reported by Tomishima and Enquist (28).

Furthermore, in our studies, a serendipitous advantage of using the in vitro chamber system was that the site of imaging was several millimeters from the SCG explant, automatically forcing us to image in the mid-distal axon instead of the prox-

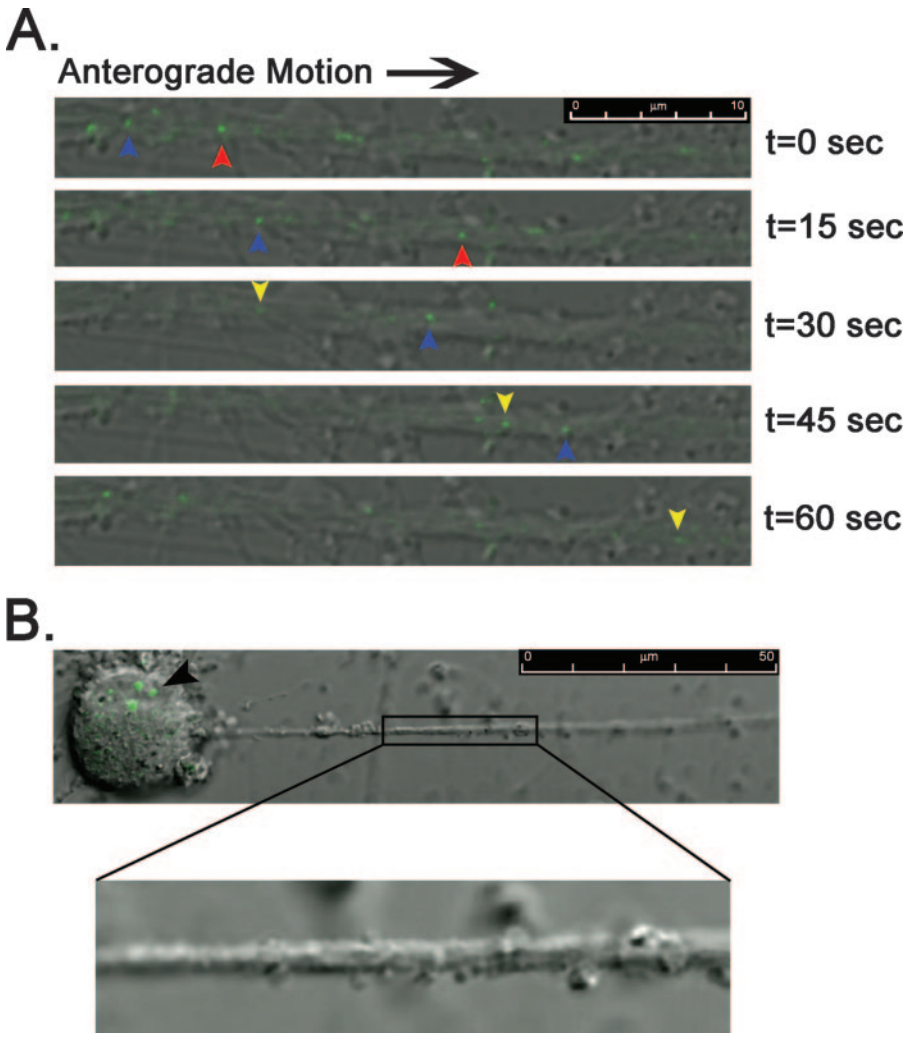

FIG. 5. Live-cell imaging of GFP-tagged capsid viruses. Dissociated SCG neurons were plated on glass-bottom MatTek dishes and allowed to differentiate for 2 weeks. Images are merged overlays of differential interference contrast and GFP. A minimum of 30 infected neurons per virus were examined for the presence of capsid puncta moving in the anterograde direction. In order to quantify the number of puncta undergoing axonal transport in neurons infected with PRV GS443, eight different axon shafts were imaged where capsids could be visualized moving >50 μm without dropping in and out of the plane of focus. An equal number of axons were examined for PRV 368 for the same time period. (A) Neurons were infected with PRV GS443 and imaged with the Leica SP5 confocal microscope between 13 and 14 h postinfection. Blue, red, and yellow arrowheads track the anterograde movement of individual fluorescent puncta through the field of view during a 1-min interval (see Movie S1 in the supplemental material). (B) A neuron infected for 13.5 h with PRV 368 (green capsid, Us9 null) shows robust green fluorescence in the soma (black arrowhead) but no presence of capsids in the axon (enlarged image, see Movie S2 in the supplemental material).

imal segment. In addition, live-cell imaging was also a key approach in determining the number of green capsid puncta undergoing anterograde transport, regardless of background fluorescence. Indeed, the first experiments by Smith et al. addressing anterograde transport kinetics of PRV capsids show green puncta traversing a "sea of green" in the proximal segment of chicken embryo DRG neurons (25).

Our work demonstrates that PRV Us9 is essential for the anterograde spread of infection in the rat visual system, as well as for neuron-to-cell spread in a compartmentalized chamber system (3, 10). Studies examining the closely related HSV Us9 homolog also support a role for this protein in anterograde spread of infection (19, 22). Polcicova et al. showed that an HSV Us9 mutant was severely impaired in its ability to spread from the murine eye to retinorecipient centers in the brain, as well as the anterograde circuit from the trigeminal ganglia to the mouse cornea (22). LaVail et al. concluded from studies in vivo that viral capsid and DNA failed to enter the axon in the absence of Us9, although gD and somewhat less gC were detected (19).

Our PRV Us9 data support a model in which viral capsids and membrane proteins assemble in the cell body and are trafficked together inside vesicles toward the axon terminus (5, 18, 20, 21). Recent live-cell imaging experiments examining anterograde and retrograde PRV transport using dual-color viruses expressing fluorescent capsid, tegument, and viral glycoproteins supports this notion (1). Capsids (visualized as fluorescent mRFP-VP26 puncta) moving away from the cell body were associated with the viral glycoprotein gD (visualized as fluorescent gD-GFP puncta). On the other

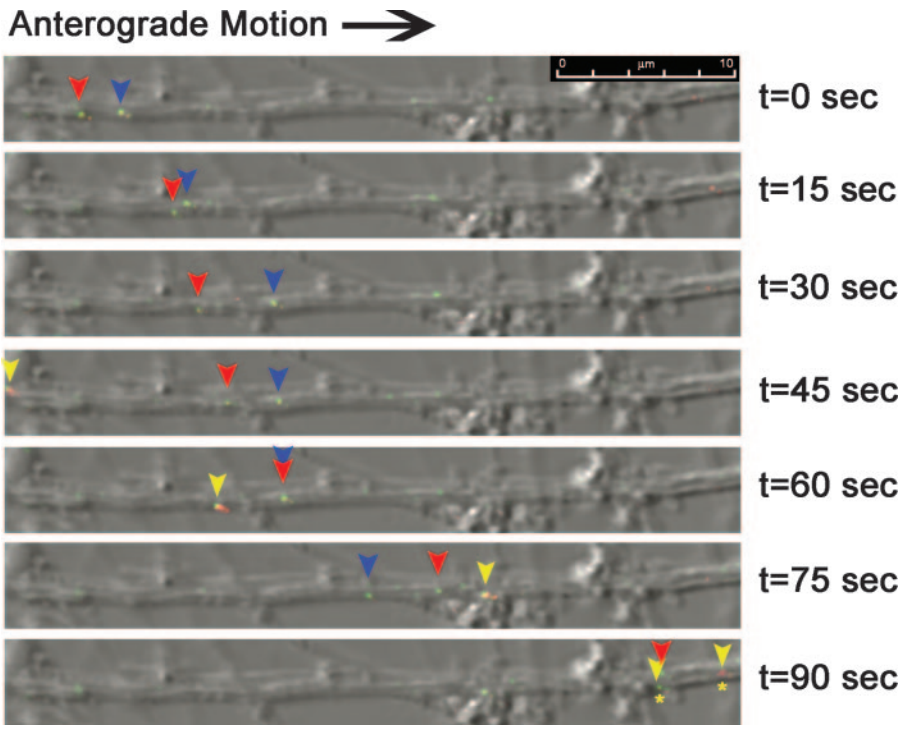

FIG. 6. Complementation of the Us9-null axonal sorting defect with PRV 180. Dissociated SCG neurons were coinfected with PRV 368 (GFP-VP26, Us9 null) and PRV 180 (RFP-VP26) and imaged on the Leica SP5 confocal microscope between 13 and 14 h postinfection. Images are merged overlays of differential interference contrast, GFP, and RFP. Blue, red, and yellow arrowheads track the anterograde movement of individual fluorescent puncta through the field of view for 1.5 min (see Movie S3 in the supplemental material). Red and blue arrowheads highlight individual yellow puncta, whose composition is a mix of GFP-VP26 and RFP-VP26. The yellow arrowhead marks a predominantly red punctum and a predominantly green punctum transported together that eventually separate. (asterisks)

hand, RFP-VP26 puncta moving toward the cell body no longer contained detectable gD-GFP but did associate with the inner tegument protein VP1/2 (1). In contrast, Snyder et al. recently concluded HSV capsids were transported in axons independent of viral membrane proteins (26). These studies were performed on fixed neurons that were subsequently stained with HSV antibodies against capsid and viral glycoproteins. This finding is also well established for PRV-infected neurons: capsid proteins and glycoproteins do not always colocalize in axons fixed and stained with antibodies (see Fig. 2 and images in references 14 and 29). In fact, this finding provided much of our initial enthusiasm for the idea that PRV structural components are trafficked separately inside the axon. However, recent reports using live-cell imaging with dual-color fluorescent PRV recombinants (1, 15), electron microscopy coupled with chamber technology (10, 11, 15), and the data from the present report indicating that PRV Us9 is required for axonal sorting of capsid and membrane proteins are more consistent with a model where assembled particles enter and move as complexes in membrane vesicles.

In summary, we report that the PRV membrane protein Us9 directly affects the axonal sorting of capsids in SCG explants and dissociated neurons. Future studies will focus on the mechanism by which Us9 mediates such axonal sorting and targeting. Our current hypothesis is that Us9 directs host transport vesicles carrying assembled virus particles to varicosities and axon termini where egress occurs. The cellular and viral proteins involved in these processes remain to be elucidated.

ACKNOWLEDGMENTS

We thank Jennifer Griffin for technical assistance with the IF and Silvia Piccinotti for providing the chamber diagrams. We also appreciate the input and advice from members of the Enquist lab.

This study was supported by the National Institute of Neurological Disorders and Stroke (grants R01 33506 and R01 33063) and the Dana Research Foundation.

ADDENDUM IN PROOF

Similar studies involving HSV gE- and US9- mutants have demonstrated that gE/gI and US9 promote anterograde transport of HSV capsids into rat and human neuronal axons (A. Snyder and D. C. Johnson, personal communication). HSV glycoprotein transport into axons was also reduced with gE- and US9- mutants, although not as severely as with capsids.

REFERENCES

1. **Antinone, S. E., and G. A. Smith.** 2006. Two modes of herpesvirus trafficking in neurons: membrane acquisition directs motion. J. Virol. **80:**11235–11240.
2. **Brideau, A. D., B. W. Banfield, and L. W. Enquist.** 1998. The Us9 gene product of pseudorabies virus, an alphaherpesvirus, is a phosphorylated, tail-anchored type II membrane protein. J. Virol. **72:**4560–4570.
3. **Brideau, A. D., J. P. Card, and L. W. Enquist.** 2000. Role of pseudorabies virus Us9, a type II membrane protein, in infection of tissue culture cells and the rat nervous system. J. Virol. **74:**834–845.
4. **Brideau, A. D., T. del Rio, E. J. Wolffe, and L. W. Enquist.** 1999. Intracellular trafficking and localization of the pseudorabies virus Us9 type II envelope protein to host and viral membranes. J. Virol. **73:**4372–4384.
5. **Card, J. P., L. Rinaman, R. B. Lynn, B. H. Lee, R. P. Meade, R. R. Miselis,**

and L. W. Enquist. 1993. Pseudorabies virus infection of the rat central nervous system: ultrastructural characterization of viral replication, transport, and pathogenesis. J. Neurosci. **13:**2515–2539.
6. **Card, J. P., L. Rinaman, J. S. Schwaber, R. R. Miselis, M. E. Whealy, A. K. Robbins, and L. W. Enquist.** 1990. Neurotropic properties of pseudorabies virus: uptake and transneuronal passage in the rat central nervous system. J. Neurosci. **10:**1974–1994.
7. **Card, J. P., M. E. Whealy, A. K. Robbins, R. Y. Moore, and L. W. Enquist.** 1991. Two alpha-herpesvirus strains are transported differentially in the rodent visual system. Neuron **6:**957–969.
8. **Ch'ng, T., E. A. Flood, and L. W. Enquist.** 2004. Culturing primary and transformed neuronal cells for studying pseudorabies virus infection, p. 299–316. *In* P. M. Lieberman (ed.), Methods in molecular biology. The Humana Press, Inc., Totoway, NJ.
9. **Ch'ng, T. H., and L. W. Enquist.** 2005. Efficient axonal localization of alphaherpesvirus structural proteins in cultured sympathetic neurons requires viral glycoprotein E. J. Virol. **79:**8835–8846.
10. **Ch'ng, T. H., and L. W. Enquist.** 2005. Neuron-to-cell spread of pseudorabies virus in a compartmented neuronal culture system. J. Virol. **79:**10875–10889.
11. **del Rio, T., T. H. Ch'ng, E. A. Flood, S. P. Gross, and L. W. Enquist.** 2005. Heterogeneity of a fluorescent tegument component in single pseudorabies virus virions and enveloped axonal assemblies. J. Virol. **79:**3903–3919.
12. **Enquist, L. W., and J. P. Card.** 2003. Recent advances in the use of neurotropic viruses for circuit analysis. Curr. Opin. Neurobiol. **13:**603–606.
13. **Enquist, L. W., P. J. Husak, B. W. Banfield, and G. A. Smith.** 1998. Infection and spread of alphaherpesviruses in the nervous system. Adv. Virus Res. **51:**237–347.
14. **Enquist, L. W., M. J. Tomishima, S. Gross, and G. A. Smith.** 2002. Directional spread of an alpha-herpesvirus in the nervous system. Vet. Microbiol. **86:**5–16.
15. **Feierbach, B., M. Bisher, J. Goodhouse, and L. W. Enquist.** 2007. In vitro analysis of trans-neuronal spread of an alpha-herpesvirus infection in peripheral nervous system neurons. J. Virol. **81:**6846–6857.
16. **Feierbach, B., S. Piccinotti, M. Bisher, W. Denk, and L. W. Enquist.** 2006. Alpha-herpesvirus infection induces the formation of nuclear actin filaments. PLoS Pathog. **2:**e85.
17. **Granzow, H., B. G. Klupp, W. Fuchs, J. Veits, N. Osterrieder, and T. C. Mettenleiter.** 2001. Egress of alphaherpesviruses: comparative ultrastructural study. J. Virol. **75:**3675–3684.
18. **Kritas, S. K., H. J. Nauwynck, and M. B. Pensaert.** 1995. Dissemination of wild-type and gC-, gE-and gI-deleted mutants of Aujeszky's disease virus in the maxillary nerve and trigeminal ganglion of pigs after intranasal inoculation. J. Gen. Virol. **76**(Pt. 8)**:**2063–2066.
19. **Lavail, J. H., A. N. Tauscher, A. Sucher, O. Harrabi, and R. Brandimarti.** 2007. Viral regulation of the long distance axonal transport of herpes simplex virus nucleocapsid. Neuroscience **146:**974–985.
20. **Lycke, E., B. Hamark, M. Johansson, A. Krotochwil, J. Lycke, and B. Svennerholm.** 1988. Herpes simplex virus infection of the human sensory neuron. An electron microscopy study. Arch. Virol. **101:**87–104.
21. **Lycke, E., K. Kristensson, B. Svennerholm, A. Vahlne, and R. Ziegler.** 1984. Uptake and transport of herpes simplex virus in neurites of rat dorsal root ganglia cells in culture. J. Gen. Virol. **65**(Pt. 1)**:**55–64.
22. **Polcicova, K., P. S. Biswas, K. Banerjee, T. W. Wisner, B. T. Rouse, and D. C. Johnson.** 2005. Herpes keratitis in the absence of anterograde transport of virus from sensory ganglia to the cornea. Proc. Natl. Acad. Sci. USA **102:**11462–11467.
23. **Pomeranz, L. E., A. E. Reynolds, and C. J. Hengartner.** 2005. Molecular biology of pseudorabies virus: impact on neurovirology and veterinary medicine. Microbiol. Mol. Biol. Rev. **69:**462–500.
24. **Smith, G. A., and L. W. Enquist.** 2002. Break ins and break outs: viral interactions with the cytoskeleton of mammalian cells. Annu. Rev. Cell Dev. Biol. **18:**135–161.
25. **Smith, G. A., S. P. Gross, and L. W. Enquist.** 2001. Herpesviruses use bidirectional fast-axonal transport to spread in sensory neurons. Proc. Natl. Acad. Sci. USA **98:**3466–3470.
26. **Snyder, A., T. W. Wisner, and D. C. Johnson.** 2006. Herpes simplex virus capsids are transported in neuronal axons without an envelope containing the viral glycoproteins. J. Virol. **80:**11165–11177.
27. **Tirabassi, R. S., and L. W. Enquist.** 2000. Role of the pseudorabies virus gI cytoplasmic domain in neuroinvasion, virulence, and posttranslational N-linked glycosylation. J. Virol. **74:**3505–3516.
28. **Tomishima, M. J., and L. W. Enquist.** 2001. A conserved alpha-herpesvirus protein necessary for axonal localization of viral membrane proteins. J. Cell Biol. **154:**741–752.
29. **Tomishima, M. J., G. A. Smith, and L. W. Enquist.** 2001. Sorting and transport of alpha herpesviruses in axons. Traffic **2:**429–436.
30. **Watson, D. H., W. C. Russell, and P. Wildy.** 1963. Electron microscopic particle counts on herpesvirus using the phosphotungstate negative staining technique. Virology **19:**250–260.
31. **Whealy, M. E., J. P. Card, A. K. Robbins, J. R. Dubin, H. J. Rziha, and L. W. Enquist.** 1993. Specific pseudorabies virus infection of the rat visual system requires both gI and gp63 glycoproteins. J. Virol. **67:**3786–3797.